Boumesbah, Allaa Eddine; Martin, Floran; Krebs, Guillaume; Belahcen, Anouar; Marchand, Claude

Comparison of Model Order Reduction Methods for a Switched Reluctance Machine Characterization

Published in:
IEEE Transactions on Magnetics

DOI:
10.1109/TMAG.2021.3059969

Published: 01/04/2021

Document Version
Peer reviewed version

Please cite the original version:
Boumesbah, A. E., Martin, F., Krebs, G., Belahcen, A., & Marchand, C. (2021). Comparison of Model Order Reduction Methods for a Switched Reluctance Machine Characterization. *IEEE Transactions on Magnetics*, *57*(4), [7400906]. https://doi.org/10.1109/TMAG.2021.3059969

Comparison of Model Order Reduction Methods for a Switched Reluctance Machine Characterization

Allaa Eddine Boumesbah[1], Floran Martin[2], Guillaume Krebs[1], Anouar Belahcen[2,3] and Claude Marchand[1]

[1] Université Paris-Saclay, CentraleSupélec, CNRS, Laboratoire de Génie Electrique et Electronique de Paris, 91192, Gif-sur-Yvette, France.
[2]Department of Electrical Engineering and Automation, Aalto University, 02150 Espoo, Finland
[3]Department of Electrical Power Engineering and Mechatronics, Tallinn University of Technology, 19086 Tallinn, Estonia

In this paper, an exhaustive comparison is presented between two types of model order reduction methods, namely the proper orthogonal decomposition (POD) and the orthogonal interpolation method (OIM), for the characterization of a switched reluctance machine. The purpose of the comparison is to find out the best practices for the design of the machine control parameters and strategy. The control design itself is not presented here, but the needed information is at the focus. The comparison is based on the computation time and the complexity of the reduced-order model as well as the accuracy of the needed data as compared with the one obtained from the full-order model. The results show that OIM is more efficient in terms of calculation time, especially when considering a nonlinear problem.

***Index Terms*—Finite element, model order reduction, orthogonal interpolation method, proper orthogonal decomposition, switched reluctance machine.**

I. Introduction

The design of electrical machines might be difficult, especially for an electrical or hybrid vehicle application. The driving cycle should be considered, and the design process requires an optimization based on a precise evaluation of the different losses created in the machine for each operating point.

The proposed characterization methodology consists of establishing flux linkage cartographies for the switched reluctance machine (SRM) using a magnetostatic finite element (FE) model. The average torque and electromotive forces can then be calculated using the flux linkage derivative. Based on these cartographies, the optimal control parameters are calculated to find the required line current waveform [1]. Finally, copper and iron losses can be calculated in a post-treatment process.

The SRM is a rotating electrical machine with nonlinear materials; the SRM model must include the nonlinear behavior of the machine and rotation aspects as they strongly affect this nonlinearity. The use of the FE method ensures a high precision; however, it can be prohibitively costly in terms of computational time, especially when dealing with a nonlinear problem [2], [3]. One solution to reduce the computation time could be using model order reduction methods (MOR).

MOR methods are used to build a reduced-order model from collected data derived from the original full-order model's solutions. This model, which is more economical in terms of calculation time, must offer acceptable accuracy. Among many MOR techniques that have been used to solve electromagnetic problems are the Proper Orthogonal Decomposition (POD) [4]-[8], the Proper Generalized Decomposition (PGD) [9]-[12], the Discrete Empirical Interpolation Method (DEIM) [13]-[16], the Best Point Interpolation Method (BPIM) [17] and the Orthogonal Interpolation Method (OIM) [18]. A POD approach for solving multiple-input problems is also presented in [19] and [20].

In this work, the focus is on the POD and the OIM techniques. The other methods have been problematic, the choice of the interpolation nodes by the DEIM does not guarantee the best precision [17], and the method can lead to numerical instabilities [16]. The BPIM has a better choice of interpolation nodes; however, it results in a higher calculation time [17]. While the PGD has significant issues when dealing with nonlinearity [21].

The POD is a classical MOR technique that has proven its effectiveness in solving linear problems. However, some drawbacks have been noted; especially when dealing with nonlinear problems, in the presence of nonlinearities, it is necessary to use the full-order model at each step of the iterative scheme to calculate the nonlinear term. The calculation time is considerably impacted by this issue [16], [17]. On the other hand, the OIM is an interpolation-based method that avoids the additional calculation time due to the evaluation of the nonlinear term [18], as it does not require access to the full order system of equations and it is non-intrusive.

In this paper, a comparison between the POD and the OIM performances is given, using single and multiple input approaches to establish fast cartographies for a switched reluctance machine (SRM) characterization. The original FE model is presented in Section II. The study case is presented in section III. The POD and the OIM reduced-order models are presented in section IV. Results obtained using the two MOR methods with a single input and multiple inputs approaches are presented in section V. A detailed analysis of the results is carried out in section VI according to the criteria of calculation time and complexity of the problem. Finally, conclusions and research perspectives are presented in section VII.

II. Finite Element Model

The governing equations for the SRM nonlinear FE model are derived from Maxwell's equations. The magnetostatic formulation is given by:

$$\boldsymbol{curl}\left(\nu\, \boldsymbol{curl}(\boldsymbol{A})\right) = \boldsymbol{J_s} \tag{1}$$

where ν is the reluctivity, $\boldsymbol{A}$ the magnetic vector potential and $\boldsymbol{J_s}$ the source current density.

The discretized nonlinear 2D FE model can be expressed by:

$$\boldsymbol{S}.\boldsymbol{X} = \boldsymbol{F} \quad (2)$$

where $\boldsymbol{X}$ is the vector of unknowns which corresponds to the z-component of the magnetic vector potential of size $n \times 1$, $\boldsymbol{S}$ the stiffness matrix of size $n \times n$, which depends on the magnetic vector potential solution and $\boldsymbol{F}$ the source vector of size $n \times 1$.

The nonlinear behavior of the magnetic material is considered in the reluctivity term and the nonlinear problem is solved using a Newton-Raphson iterative scheme, as in (3):

$$\boldsymbol{J}\,\Delta\boldsymbol{X}^i = -\boldsymbol{R}(\boldsymbol{X}^{i-1}) \quad (3)$$

The residual vector $\boldsymbol{R}$ and the Jacobean matrix $\boldsymbol{J}$ are given by:

$$\boldsymbol{R}(\boldsymbol{X}) = \boldsymbol{S}(\boldsymbol{X})\boldsymbol{X} - \boldsymbol{F} \quad (4)$$

$$\boldsymbol{J}(\boldsymbol{X}) = \partial\boldsymbol{R}(\boldsymbol{X})/\partial\boldsymbol{X} \quad (5)$$

Whereas the rotation is modeled using the moving band technique [22].

III. Study Case

The study case is a 12/8 SRM of 10 kW (Fig. 1. a), meshed with 8031 first-order elements (Fig. 1. b), the number of nodes is 4478. The parameters of the machine are listed in Table 1.

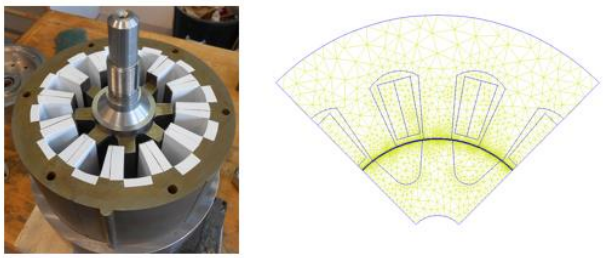

(a) (b)

Fig. 1. The studied machine (a) and associated mesh (b).

TABLE I
Parameters of the Studied Machine

Parameter	Value
Power	10 kW
Stator outer diameter	225 mm
Stator inner diameter	105 mm
Air gap thickness	0.5 mm
Shaft diameter	30 mm
Active length	120 mm

The FE model in (2) is solved to obtain, from the magnetic vector potential, the mapping of the machine phase flux as a function of the rotor position and phase currents. It can be used to elaborate the optimized control laws of the machine for a variable speed application as illustrated in Fig. 2. This mapping can be then used for geometrical structure optimization [23].

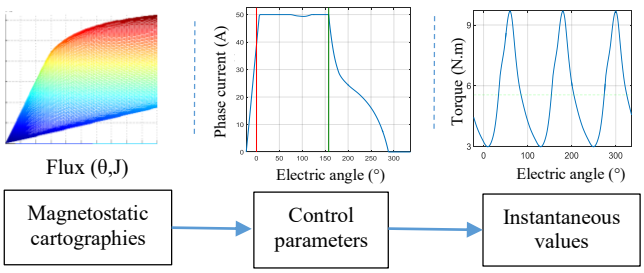

Fig. 2. Application methodology.

A fine discretization of the input variables, i.e. position (rotation angle (θ)) and current levels (current density (J)), results in considerable calculation times that must be reduced.

IV. Model Order Reduction Methods

MOR methods allow creating a reduced-order model based on data gathered from the original FE model using the method of snapshots [24]. It performs an interpolation or a reduced solution based on a limited number of solutions of the original model.

A snapshot matrix $\boldsymbol{M_s}$ of size $n \times m$ is created by solving the FE model in (2) for m selected operation points corresponding to different inputs in terms of currents and positions. The choice of these snapshots will be discussed in the following section.

$$\boldsymbol{M_s} = ([\boldsymbol{X}]_1 \quad \cdots \quad [\boldsymbol{X}]_m) \quad (6)$$

m is the number of snapshots and $[\boldsymbol{X}]_i$ is the full model solution at the i^{th} selected operation point.

The snapshot matrix is then decomposed using the singular value decomposition (SVD), as in (7):

$$\boldsymbol{M_s} = \boldsymbol{Y}\boldsymbol{\Sigma}\boldsymbol{W}^t \quad (7)$$

where $\boldsymbol{Y}$ is the left singular vectors matrix of size $n \times n$, $\boldsymbol{W}$ the right singular vectors matrix of size $m \times m$ and $\boldsymbol{\Sigma}$ a diagonal matrix of size $n \times m$, composed by the singular values of $\boldsymbol{M_s}$.

Different reduced-order models are built from the data stored in the snapshot matrix, following the used MOR method. The usage of the snapshot matrix in different methods is explained in more details in the next sub-sections.

A. Proper orthogonal decomposition method

A discrete projection operator $\boldsymbol{\Psi}$ of size $n \times m$, is obtained using the left singular vectors:

$$\boldsymbol{\Psi} = \boldsymbol{Y}\boldsymbol{\Sigma} \quad (8)$$

The solution $\boldsymbol{X}$ of (2) can then be approximated by a reduced solution vector $\boldsymbol{X_r}$ of size m, using the discrete projection operator:

$$\boldsymbol{X} = \boldsymbol{\Psi}\,\boldsymbol{X_r} \quad (9)$$

The reduced-order model is obtained by substituting (9) into (2):

$$\boldsymbol{S_r}\boldsymbol{X_r} = \boldsymbol{F_r} \quad (10)$$

where $\boldsymbol{S_r}$ is the reduced stiffness matrix of size $m \times m$ and $\boldsymbol{F_r}$ the reduced source vector of size m, given by:

$$\boldsymbol{S_r} = \boldsymbol{\Psi}^t\boldsymbol{S}\boldsymbol{\Psi} \quad (11)$$

$$\boldsymbol{F_r} = \boldsymbol{\Psi}^t\boldsymbol{F} \quad (12)$$

The reduced residual vector $\boldsymbol{R_r}$ and the reduced Jacobean matrix $\boldsymbol{J_r}$, are given by:

$$\boldsymbol{R_r}(\boldsymbol{\Psi X_r}) = \boldsymbol{\Psi}^t \boldsymbol{R}(\boldsymbol{\Psi X_r}) \quad (13)$$

$$\boldsymbol{J_r}(\boldsymbol{\Psi X_r}) = \boldsymbol{\Psi}^t \boldsymbol{J}(\boldsymbol{\Psi X_r})\boldsymbol{\Psi} \quad (14)$$

Reduced-order nonlinear terms in (13) and (14) still depend on the full-order solution. For the calculation of the nonlinear terms, the full-order stiffness matrix is assembled at each step of the Newton-Raphson iteration, which results in a time-consuming operation.

B. Orthogonal interpolation method

OIM is a straightforward interpolation-based MOR method that uses the right singular vectors of the snapshot matrix. Interpolation is performed on the right singular vectors matrix W resulting from the SVD in (7).

The matrix W is composed of singular vectors, each column of W^t corresponds to a specific input (a current density and a rotation angle) from the selected inputs for the snapshots [17], as in (15):

$$\boldsymbol{M_s} = \begin{pmatrix} x_{11} & \cdots & x_{1m} \\ \vdots & \ddots & \vdots \\ x_{m1} & \cdots & x_{mm} \\ \uparrow & & \uparrow \\ p_1 & \cdots & p_m \end{pmatrix} \xrightarrow{SVD} \boldsymbol{W^t} = \begin{pmatrix} w_{11} & \cdots & w_{1m} \\ \vdots & \ddots & \vdots \\ w_{m1} & \cdots & w_{mm} \\ \uparrow & & \uparrow \\ p_1 & \cdots & p_m \end{pmatrix} \quad (15)$$

For the selected input set $\boldsymbol{p}$ for the snapshots, each column of W can be expressed as a function of $\boldsymbol{p}$:

$$\boldsymbol{W} = \begin{pmatrix} f_1(\boldsymbol{p}) & f_2(\boldsymbol{p}) & \cdots & f_m(\boldsymbol{p}) \end{pmatrix} \quad (16)$$

where $f_i(\boldsymbol{p})$ is the function that represents the i^{th} right singular vector as a function of the input set.

For any new input set $\boldsymbol{p_{new}}$, a new matrix $\boldsymbol{W_{new}}$ is obtained by interpolating each column of $\boldsymbol{W}$ for the new input set:

$$\boldsymbol{W_{new}} = \begin{pmatrix} f_1(\boldsymbol{p_{new}}) & f_2(\boldsymbol{p_{new}}) & \cdots & f_m(\boldsymbol{p_{new}}) \end{pmatrix} \quad (17)$$

A solution matrix $\boldsymbol{Sol}$ for the inputs $\boldsymbol{p_{new}}$ is then estimated by:

$$\boldsymbol{Sol} = \boldsymbol{Y \Sigma W_{new}}^t \quad (18)$$

The f_i functions represent the right singular vectors using a modified Akima interpolation [25]. Other interpolation methods could be used, such as linear or cubic interpolations. For the studied case, Akima interpolation gives a better precision.

V. Results

The two proposed MOR methods are applied to the SRM model. The application aims to establish a flux linkage cartography using the different models and discuss the performances regarding the complexity of the models and the computation time.

The flux linkage Φ through an enclosed surface with a boundary $\boldsymbol{\Gamma}$, is calculated using the magnetic vector potential $\boldsymbol{A}$:

$$\Phi = \oint_{\boldsymbol{\Gamma}} \boldsymbol{A}.\, d\boldsymbol{\Gamma} \quad (19)$$

The results obtained using the full order model are taken as a reference and the results from the reduced models are compared to this reference. As the purpose of the study is to evaluate the performances of the MOR models, the number of snapshots is chosen using an iterative scheme to determine the lowest possible number to ensure a mean absolute error on the flux e_m lower than 1%.

The local error for the i^{th} input is calculated by:

$$e^i = \frac{\left|\Phi^i_{full} - \Phi^i_{reduced}\right|}{\left|\Phi^i_{full}\right|} \times 100 \quad (20)$$

where Φ^i_{full} is the flux linkage calculated at the i^{th} input using the full order model and $\Phi^i_{reduced}$ the flux linkage calculated at the i^{th} input using the reduced-order model. The global error is the mean of the local errors for the different inputs:

$$e_m = \frac{\sum_{i=1}^{nc} e^i}{nc} \quad (21)$$

where nc is the total number of inputs.

For each model, calculation time and error are evaluated. For each model, first the total calculation time is given, including the time required to calculate the snapshots, build and solve the reduced order model. Then, the snapshots calculation time and the time required to solve the reduced order model are given separately.

A. Full order model

A cartography (Fig. 3.) is created by calculating the magnetic flux Φ across one phase, for 24 rotation angles θ from 0° to 23° by a step of 1° and 51 current densities J from 0 A/mm^2 to 5 A/mm^2 by a step of 0.1 A/mm^2. The position $\theta = 0°$ corresponds to the aligned position as in Fig. 1. b and the position $\theta = 23°$ corresponds to the opposition position. The model is saturated for the high currents around the aligned position, which corresponds to a flux superior to 0.02 Wb in Fig. 3. The current density is assumed to be uniformly distributed in the slots (no skin or proximity effects) and the computation methodology is quasi-static, i.e. does not consider eddy-currents in any region of the model.

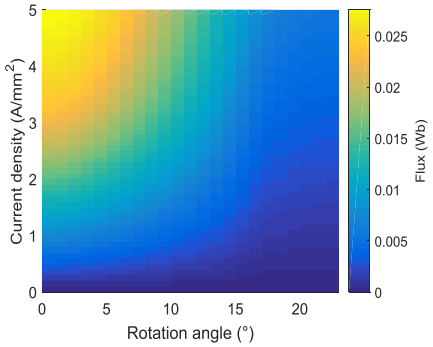

Fig. 3. Cartography of flux as a function of current density and rotation angle obtained using the full order model.

The total number of times the full model is solved is then 1224 and the calculation time necessary to establish the flux linkage cartography using the full order model is 109s, obtained using an i5 CPU with a 3.12 Go RAM, i.e. 89 ms per input pair.

The stop criterion for the Newton-Rhaphson scheme is set at 10^{-2}; the number of required iterations is 3031. Choosing a smaller stop criterion does not significantly improve the precision of the model. When using an absolute criteria of 10^{-6}, the total number of iterations is 4940, and the total calculation time is 158 s. The global error on the flux between the two criteria is 0.0094%.

Precision and convergence are also related to the mesh; when

using an extremely fine mesh with 80215 elements, the total calculation time is 1439 s, the global error induced by the mesh on the flux is 0.34%.

MOR models will be used in order to reduce the calculation time of the flux linkage cartography. Different approaches can be considered as follows.

B. Single input approach

Although depending on both the current density J and rotor position θ, the problem could be subdivided into several single input problems by fixing one of the two mentioned parameters. In this case, several reduced-order models can be built, with each one only valid for a limited number of operating points.

For the single input approach, θ is fixed, and the problem is simplified to the flux linkage as a function of the current density $\Phi(J)$. By fixing θ, the reduced-order model can only be used for the selected value of θ, which means that instead of selecting snapshots that scan the whole operating range and create a single reduced-order model, different sets of snapshots are selected for each θ, and a new reduced-order model is built for each θ.

Current density could be fixed instead of rotor position; however, fixing θ results in lower calculation time.

For each rotation angle, m snapshots are taken by selecting m currents while θ is fixed. A new reduced-order model is built for each rotor position as illustrated in Fig. 4.

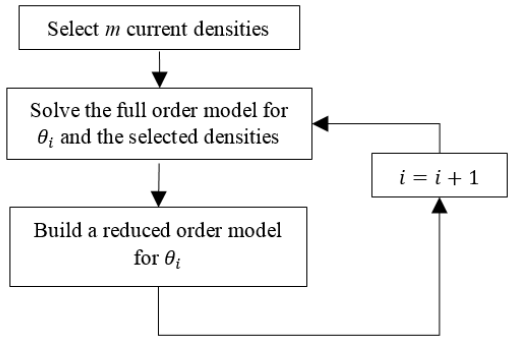

Fig. 4. Single input approach algorithm flowchart.

The single input approach is applied using both POD and OIM models.

1) POD model

The flux linkage cartography is now calculated using the POD model with the single input approach. A single snapshot is taken for each rotation angle ($m = 1$), which makes a total of 23 snapshots. The selected current density is $5\ A/mm^2$ for every rotation angle, any other value can be chosen instead of $5\ A/mm^2$, since the number of snapshots is always the same (one snapshot), the global error will not change considerably and only the error distribution will be affected. The process results in 23 reduced-order models (one for each rotation angle) of one unknown. Since the POD is not an interpolation-based method, a reduced order model could be built using a single snapshot. The nonlinear behavior is preserved by the calculation of the full-order stiffness matrix at each Newton-Raphson iteration. The error distribution from this approach is presented in Fig. 5.

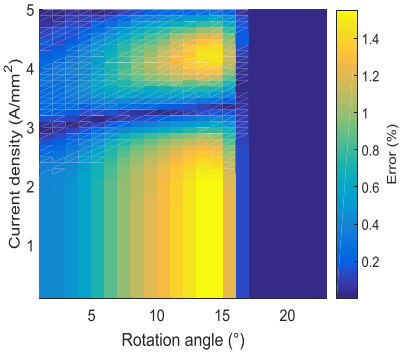

Fig. 5. Error distribution for the POD single input model.

The POD single input model allows the creation of the flux linkage cartography in 72s, of which 3s are required to calculate the snapshots, and 42s are required to solve the reduced-order models i.e. equation (10). By taking 23 snapshots, the global error on the flux linkage cartography is evaluated at 0.5%. Although, locally, a maximal error of 1.55% is recorded.

As shown in Fig. 5. the error is lower for the position from 16 to 23, where the flux linkage has a linear behavior, as these positions are situated around the opposition position.

2) OIM model

Using the OIM model with a single input approach, 4 uniformly distributed snapshots for each rotation angle are required to satisfy the desired accuracy, making a total of 92 snapshots. A reduced-order model of 4 unknowns is built for each position.

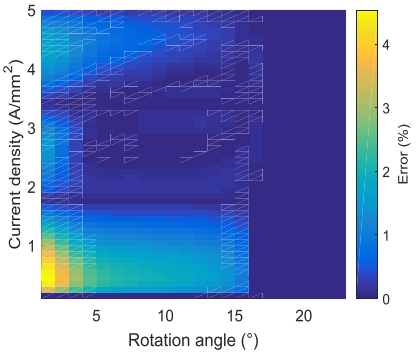

Fig. 6. Error distribution for the OIM single input model.

The total calculation time is 19s, including 7s to calculate the snapshots and only 0.38s to solve the reduced-order model i.e. equations (17) and (18). The global error is 0.41%, and the maximal local error is 4.53%. As shown in Fig. 6. the highest errors are recorded for low current densities. Since the calculated errors are relative, a 4.5% error does not reflect the model's accuracy.

C. Multiple inputs approach

A second approach consists of considering the problem as a two inputs problem. In this case, the interpolation's target function is the flux linkage as a function of both current density and rotor position $\Phi(J, \theta)$.

A set of inputs is selected, m_J current densities and m_θ rotation angles, to get a total of $m_J \times m_\theta$ snapshots. A more

complex but a single reduced-order model is built for the whole working range as illustrated in Fig. 7.

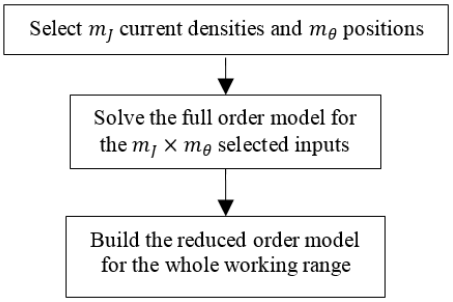

Fig. 7. Multiple input approach algorithm flowchart.

1) POD model

When using the multiple-input approach, only 12 snapshots are required to get the same order of accuracy. The snapshots are taken by selecting one current density ($m_J = 1$) and 12 rotation angles ($m_\theta = 12$) uniformly distributed. The process results in a single global reduced-order model of 12 unknowns. Error distribution is presented in Fig. 8.

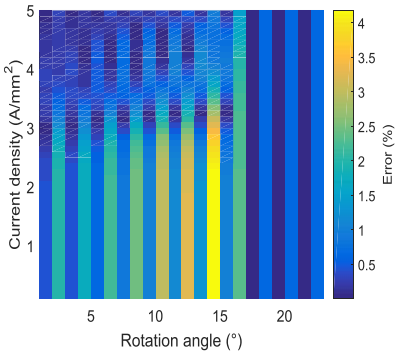

Fig. 8. Error distribution for the POD multiple inputs model.

The total calculation time is evaluated at 69s, the 12 snapshots are calculated in 1.5s using the full order model and the reduced-order model in (10) is solved in 42s. The global error on the flux linkage cartography is 0.94%. Locally, the maximal error is 4.18%. Error distribution (Fig. 8.) is explained by the fact that snapshots are not taken for every rotation angle. Therefore, the local error is higher for positions where no data was considered for creating the reduced-order model.

2) OIM model

Using the multiple-input approach, the OIM model requires 32 snapshots gathered by selecting 4 current densities and eight rotation angles ($m_J = 4$ and $m_\theta = 8$). A single reduced-order model is built with 32 unknowns.

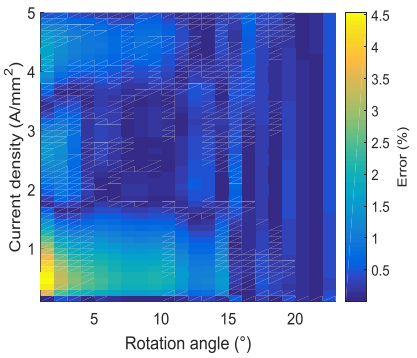

Fig. 9. Error distribution for the OIM multiple inputs model.

The total computation time is 7.4s, divided on 2.3s required for the snapshots calculation and only 0.06s required for solving the reduced-order model represented by the equations (17) and (18). The global error on the flux linkage cartography is evaluated at 0.5%, while the maximal local error is 4.54%. Error distribution (Fig. 9.) shows that the highest errors are recorded for the lowest current densities.

VI. COMPARISON

The results obtained using the four MOR approaches and the full order model are summarized in Table 2. n and m being the number of unknowns and the total number of snapshots, respectively.

TABLE II
RESULTS SUMMARY

Method	n	m	Total time (s)	Generation time (s)	Solving time (s)
Full order	4478	/	109	24	85
POD single	1	23	72	30	42
POD multiple	12	12	69	27	42
OIM single	4	92	19	18.6	0.38
OIM multiple	32	32	7.4	7.34	0.06

MOR methods have significantly reduced the order of the original model. The OIM models are more complex than the POD models and require more snapshots to get the same accuracy. However, since the method has a straightforward application, the time required to solve the OIM models is far lower than that required to solve the POD models. Globally, even if the OIM requires a higher number of snapshots, the total computation time is significantly lower for OIM models.

The single input approach results in lower-order models; however, since several reduced-order models are required, the total computation time is higher than when using a multiple inputs approach.

The OIM multiple inputs model is the most efficient model among those studied, allowing the creation of cartographies in 7s. This model could be used in the SRM design process, as control parameters optimization and the evaluation of losses depend on magnetostatic flux and torque cartographies.

VII. CONCLUSION

A comparison is made between POD and OIM MOR methods, using a single input and multiple inputs approaches.

An application to establish flux linkage cartography for a switched reluctance machine had shown the efficiency of the OIM models. The OIM requires more snapshots than the POD and results in a more complex reduced-order model. However, when using a multiple inputs approach OIM model is 14 times faster than the full order model and nine times faster than the POD model. Establishing fast cartographies will reduce the necessary time to optimize control laws, thus reducing the design process's total time. In future works, the OIM multiple inputs model will be integrated into the SRM design process, to include the copper losses analysis for a winding optimization.

REFERENCES

[1] A. Kolli, G. Krebs, X. Mininger and C. Marchand, "Impact of command parameters on efficiency, torque ripple and vibrations for Switched Reluctance motor," *2012 XXth International Conference on Electrical Machines*, Marseille, 2012, pp. 2975-2980.

[2] G. Y. Sizov, D. M. Ionel and N. A. O. Demerdash, "A review of efficient FE modeling techniques with applications to PM AC machines," *2011 IEEE Power and Energy Society General Meeting*, Detroit, MI, USA, pp. 1-6, 2011.

[3] W. N. Fu, S. L. Ho, H. L. Li and H. C. Wong, "An effective method to reduce the computing time of nonlinear time-stepping finite-element magnetic field computation," *IEEE Transactions on Magnetics*, vol. 38, no. 2, pp. 441-444, March 2002.

[4] Y. Zhai and L. Vu-Quoc, "Analysis of power magnetic components with nonlinear static hysteresis: proper orthogonal decomposition and model reduction," *IEEE Transactions on Magnetics*, vol. 43, no. 5, pp. 1888-1897, May 2007.

[5] D. Schmidthausler and M. Clemens, "Low-order electroquasistatic field simulations based on proper orthogonal decomposition," *IEEE Transactions on Magnetics*, vol. 48, no. 2, pp. 567-570, Feb. 2012.

[6] Y. Sato and H. Igarashi, "Model reduction of three-dimensional eddy current problems based on the method of snapshots," *IEEE Transactions on Magnetics*, vol. 49, no. 5, pp. 1697-1700, May 2013.

[7] T. Shimotani, Y. Sato and H. Igarashi, "Equivalent-circuit generation from finite-element solution using proper orthogonal decomposition," *IEEE Transactions on Magnetics*, vol. 52, no. 3, pp. 1-4, March 2016.

[8] M. Farzamfar, P. Rasilo, F. Martin and A. Belahcen, "Proper orthogonal decomposition for order reduction of permanent magnet machine model," *2015 18th International Conference on Electrical Machines and Systems (ICEMS)*, Pattaya, pp. 1945-1949, 2015.

[9] T. Henneron and S. Clénet, "Model order reduction of quasi-static problems based on POD and PGD approaches," *The European Physical Journal Applied Physics*, vol. 64, no 2, pp. 24514, 2013.

[10] T. Henneron and S. Clénet, "Proper generalized decomposition method applied to solve 3-D magnetoquasi-static field problems coupling with external electric circuits," *IEEE Transactions on Magnetics*, vol. 51, no. 6, pp. 1-10, June 2015.

[11] M. Pineda-Sanchez, F. Chinesta, J. Roger-Folch, M. Riera-Guasp, J. Pérez-Cruz and al. "Simulation of skin effect via separated representations," *COMPEL-The international journal for computation and mathematics in electrical and electronic engineering*, pp. 919-929, 2010.

[12] T. Henneron and S. Clénet, "Application of the proper generalized decomposition to solve magnetoelectric problem," *IEEE Transactions on Magnetics*, vol. 54, no. 3, pp. 1-4, March 2018.

[13] T. Henneron and S. Clénet, "Model order reduction of non-linear magnetostatic problems based on POD and DEI methods," *IEEE Transactions on Magnetics*, vol. 50, no. 2, pp. 33-36, Feb. 2014.

[14] D. Klis, O. Farle and R. Dyczij-Edlinger, "Model-order reduction for the finite-element boundary-element simulation of Eddy-current problems including rigid body motion," *IEEE Transactions on Magnetics*, vol. 52, no. 3, pp. 1-4, March 2016.

[15] Y. Sato, M. Clemens and H. Igarashi, "Adaptive subdomain model order reduction with discrete empirical interpolation method for nonlinear magneto-quasi-static problems," *IEEE Transactions on Magnetics*, vol. 52, no. 3, pp. 1-4, March 2016.

[16] L. Montier, A. Pierquin, T. Henneron and S. Clénet, "Structure preserving model reduction of low-frequency electromagnetic problem based on POD and DEIM," *IEEE Transactions on Magnetics*, vol. 53, no. 6, pp. 1-4, June 2017.

[17] T. Henneron, L. Montier, A. Pierquin and S. Clénet, "Comparison of DEIM and BPIM to speed up a POD-based nonlinear magnetostatic model," *IEEE Transactions on Magnetics*, vol. 53, no. 6, pp. 1-4, June 2017.

[18] M. Farzam Far, F. Martin, A. Belahcen, L. Montier and T. Henneron, "Orthogonal interpolation method for order reduction of a synchronous machine model," *IEEE Transactions on Magnetics*, vol. 54, no. 2, pp. 1-6, Feb. 2018.

[19] T. Henneron and S. Clénet, "Model-order reduction of multiple-input non-linear systems based on POD and DEI methods," *IEEE Transactions on Magnetics*, vol. 51, no. 3, pp. 1-4, March 2015.

[20] M. Farzamfar, A. Belahcen, P. Rasilo, S. Clénet and A. Pierquin, "Model order reduction of electrical machines with multiple inputs," *IEEE Transactions on Industry Applications*, vol. 53, no. 4, pp. 3355-3360, July-Aug. 2017.

[21] T. Henneron, A. Benabou and S. Clenet, "Nonlinear proper generalized decomposition method applied to the magnetic simulation of a SMC microstructure," in IEEE Transactions on Magnetics, vol. 48, no. 11, pp. 3242-3245, Nov. 2012.

[22] H. De Gersem, J. Gyselinck, P. Dular and al. "Comparison of sliding-surface and moving-band techniques in frequency-domain finite-element models of rotating machines," *COMPEL-The international journal for computation and mathematics in electrical and electronic engineering*, vol. 23, no 4, pp. 1006-1014, 2004.

[23] G. Krebs, E. de Cecco and C. Marchand, "Design approach of an axial flux motor for electrical powertrain vehicle," *2012 XXth International Conference on Electrical Machines, Marseille*, pp. 2812-2817, 2012.

[24] L. Sirovich, "Turbulence and the dynamics of coherent structures. I. Coherent structures," *Quarterly of applied mathematics*, vol. 45, no 3, pp. 561-571, 1987.

[25] H. Akima, "A new method of interpolation and smooth curve fitting based on local procedures," *Journal of the ACM (JACM),* vol. 17, no 4, p. 589-602, 1970.